INSTITUTE OF PHYSICS PUBLISHING JOURNAL OF PHYSICS: CONDENSED MATTER

J. Phys.: Condens. Matter **16** (2004) S5345–S5370 PII: S0953-8984(04)75603-9

Water in nanopores: II. The liquid–vapour phase transition near hydrophobic surfaces

Ivan Brovchenko[1], **Alfons Geiger**[1] **and Alla Oleinikova**[2]

[1] Physical Chemistry, Dortmund University, 44221 Dortmund, Germany
[2] Physical Chemistry, Ruhr-University Bochum, 44780 Bochum, Germany

E-mail: brov@heineken.chemie.uni-dortmund.de, alfons.geiger@udo.edu and alla.oleinikova@ruhr-uni-bochum.de

Received 31 January 2004
Published 29 October 2004
Online at stacks.iop.org/JPhysCM/16/S5345
doi:10.1088/0953-8984/16/45/004

Abstract

The liquid–vapour phase transition near a weakly attractive surface is studied by simulations of the coexistence curves of water in hydrophobic pores. There is a pronounced gradual density depletion of the liquid phase near the surface without any trend to the formation of a vapour layer below the bulk critical temperature T_C. The temperature dependence of the order parameter in the surface layer follows the power law $(\rho_l - \rho_v) \sim (1 - T/T_C)^{\beta_1}$ with a value of the exponent β_1 close to the critical exponent $\beta_1 = 0.82$ of the *ordinary* transition in the Ising model. The order parameter profiles in the subcritical region are consistent with the behaviour of an ordinary transition and their temperature evolution is governed by the bulk correlation length. Density profiles of water at supercritical temperatures are consistent with the behaviour of the *normal* transition caused by the preferential adsorption of voids. The relation between normal and ordinary transitions in the Ising model and in fluids is discussed.

1. Introduction

Studies of the water behaviour near hydrophobic surfaces are necessary for the understanding of various phenomena: hydrophobic attraction between extended surfaces, slipping flow of liquid water near a hydrophobic surface, hydrophobic interaction between large solutes in aqueous solutions, etc. In particular, the hydrophobic interaction plays an important role in the processes of protein folding. The ultimate prerequisite of such studies is the knowledge of the phase behaviour of water near the surface, that includes surface critical behaviour and location of the surface phase transitions.

In the case of a weak fluid–wall interaction a drying transition, i.e. the formation of a macroscopically thick vapour layer near the surface in the liquid phase, could be expected in

general, similar to the wetting transition in the case of a strong fluid–wall interaction [1–4]. For a fluid near a hard wall a drying transition, which is accompanied by the formation of a liquid–vapour interface at some distance from the substrate, is expected [5]. The possible appearance of a vapour layer around hard spheres in liquid water was also discussed [6, 7]. In simulations a drying-like surface phase transition in the liquid phase of water near a substrate with a repulsive step in the interaction potential was found [8]. For a weakly attractive *short-range* fluid–wall interaction a drying transition, as expected from general theoretical arguments [2, 3], was reported for Lennard-Jones (LJ) fluids [9, 10]. In the case of a *long-range* fluid–wall interaction (for example, via van der Waals forces) a drying transition takes place at the bulk critical temperature only [11–13]. This means that a macroscopic vapour layer between the liquid and the surface probably never occurs in real systems. Indeed, a drying transition was never observed experimentally. The absence of a drying transition also eliminates the possibility to observe predrying transitions in the stable liquid states, which means the formation of a thin vapour layer in states outside the liquid–vapour coexistence region.

The presence of a solid boundary affects the critical behaviour of a fluid. This in turn determines the properties of the fluid not only near the critical point but in a wider range of the thermodynamic conditions. The fluid becomes heterogeneous and the local properties, including the density, depend on the distance to the surface. The behaviour of the local properties near the surface should follow the laws of some surface universality class. The bulk fluid belongs to the universality class of the 3D Ising model, which shows three surface universality classes, depending on the interaction with the surface and the interparticle interaction in the surface layer [14]. In fluids, the average intermolecular interaction energy per particle always diminishes near the surface due to the effect of missing neighbours and, therefore, only two universality classes may be relevant: the so-called ordinary and normal transitions.

In a zero surface field $h_1 = 0$ (free boundary), the effect of missing neighbours results in the *ordinary* transition universality class behaviour [15, 16]. The order parameter (magnetization $|m|$ in the case of the Ising model) in both coexisting phases significantly decreases towards the surface at temperatures T below the critical temperature T_C, and its profile becomes flat ($m = 0$) at T_C and in the supercritical region. The temperature dependence of the order parameter in the surface layer m_1 follows the scaling law [15]

$$m_1 = \pm B_1 \tau^{\beta_1}, \tag{1}$$

where $\tau = (T_C - T)/T_C$ is the reduced temperature, and $\beta_1 \approx 0.82$ [17] is the surface critical exponent, which is considerably higher than the bulk critical exponent $\beta \approx 0.326$ [18].

A non-zero surface field $|h_1| > 0$ causes preferential adsorption of one of the components and a behaviour according to the *normal* transition universality class. In such a case the magnetization profile does not vanish at $T \geqslant T_C$ and the deviation of the magnetization from the bulk value increases toward the surface. In fluids this effect causes the phenomenon of critical adsorption [19]. The surface critical behaviour in the limit $|h_1| \to \infty$ is equivalent to the so-called *extraordinary* transition, which occurs when the interaction between the spins in the surface layer exceeds some critical value [20]. Although in the case of a normal transition the magnetizations of the coexisting phases are not symmetrical relative to the axis $m = 0$, the difference of magnetizations approaches a flat profile $\Delta m(z) = 0$, when $T \to T_C$, similar to the ordinary transition (and contrary to the extraordinary transition [14]). For the normal and extraordinary transitions the magnetization in the surface layer is predicted to show the following temperature dependence [20]:

$$m_1 = (m_{1C} + A_1\tau + A_2\tau^2 + \cdots) + B_\pm \tau^{2-\alpha}, \tag{2}$$

where the contribution in parentheses is a regular background, while the leading singular contribution is $\sim\tau^{2-\alpha}$ ($\alpha \approx 0.11$ [18]), when approaching T_C from below (B_-) or above (B_+). Note that the singular contribution becomes negligible compared to the linear regular term when $T \to T_C$.

In the general case $|h_1| < \infty$ the magnetization profile at $T = T_C$ shows a maximum at some distance from the surface. This maximum increases and approaches the surface when $|h_1| \to \infty$, while it moves away from the surface and disappears when $|h_1| \to 0$ [21, 22]. Such behaviour corresponds to the crossover of the critical behaviour from ordinary transition near the surface to normal transition away from it, where the crossover distance approximately coincides with the maximum of the magnetization at $T = T_C$. This means that in a surface layer the critical behaviour corresponding to the normal transition could be observed in the limit of strong adsorption only.

In so far as a fluid belongs to the same universality class as the 3D Ising model, it is natural to map the surface critical behaviour of fluids to the surface universality classes described above. In liquid binary mixtures the interaction of both components with the surface is attractive, and the condition $|h_1| = 0$ in the Ising model is fulfilled at some non-zero liquid–surface interaction potential [23]. So, binary mixtures belong to the universality class of normal transition in the sense that they show preferential adsorption of one component ($|h_1| \neq 0$). Nevertheless, experimental studies show that the behaviour of the local order parameter, i.e. the difference between the concentrations of the coexisting phases near the surface at $T < T_C$, follows a power law with the critical exponent of an ordinary transition, at least in the case of a weak preferential adsorption [24, 25]. The crossover from ordinary to normal transition, predicted for the Ising model [21], was confirmed experimentally for supercritical binary mixtures [26], and a crossover distance up to dozens of nanometers was obtained for weak preferential adsorption.

The surface critical behaviour in a one-component fluid is essentially less clear in comparison with binary mixtures. Interaction with the surface and the effect of missing neighbours near the surface are physically meaningful for real molecules. The only possible definition of the second component as being represented by the voids introduces a drastic asymmetry of the system, because this 'component' does not show any interaction, effect of missing neighbours, etc. This makes it difficult to define the order parameter properly and to find the strength of the fluid–surface attraction, which provides the condition for the ordinary transition ($|h_1| = 0$). For example, this condition may be attributed to the horizontal density profile of critical fluids [27]. This could be achieved at some definite attractive fluid–wall interaction. Further strengthening of fluid–wall interaction causes preferential adsorption of molecules. Note that in this regime a crossover from ordinary to normal transition with the distance to the wall for an LJ fluid was found [27]. To our knowledge, there are no experimental studies of the surface critical exponent of the order parameter in a one-component fluid. The only simulation study was reported for water near a hydrophobic surface, where the value of the exponent β_1 was found to be close to the Ising value for an ordinary transition [28].

Surface transitions as well as the surface critical behaviour are modified in the cases of more than one confining surface and (or) non-planar surfaces (for example, in the case of fluids in pores or large solutes and colloids in fluids). The phase transition of a fluid in a pore is shifted with respect to the bulk one in the μ–T plane (see the brief review in the first paper [29] of this series). This distorts the surface phase transitions [4, 30] as well as the surface critical behaviour. The local critical behaviour depends strongly on the particular shape of the surface (corners, edges, cones, cubes, parabolic surfaces, etc) both in the cases of ordinary and normal transitions [31–34]. As a result, the critical surface exponent becomes non-universal, i.e. dependent on the system shape. In some cases, for example for parabolic surfaces, the surface critical behaviour is no longer characterized by the usual power laws but by stretched exponentials [34].

For experimental and computer simulation studies of the surface transition and surface critical behaviour in one-component systems, the fluid density distribution near the surface is the key property. Experimental studies of the liquid density near solid surfaces show oscillations [35, 36] and depletion [13, 36–41]. Noticeable depletion of the liquid water density near various hydrophobic surfaces was detected by neutron reflectivity [37–39], x-ray reflectivity [40] and electric conductivity [41] measurements. Liquid water density of about 85–90% of the bulk value was found in the interval of 20–50 Å from the surface by neutron reflectivity measurements [37–39]. These experiments did not allow water density profiles to be obtained, but they clearly indicate the absence of a macroscopic vapour layer at a surface. The density profiles obtained from x-ray reflectivity measurements of water at a paraffin surface [40] show a water density of about 90–93% of the bulk value at distances less then 15 Å from the surface. A much stronger density depletion, which appears as gradual density decay and not as formation of a vapour layer, was observed in the case of *n*-hexane at a silicon surface [36]. Note also that adsorption measurements show strong depletion of the liquid neon density near an extremely weakly attractive cesium surface when approaching the neon critical temperature [13]; however, they do not allow one to distinguish between a gradual density decay and the formation of a vapour layer.

The presence of nanobubbles at hydrophobic surfaces in water (see [42] for a recent review) may, in principle, indicate the formation of a water vapour layer. However, the amount and size of the nanobubbles decrease considerably in degassed water [38] and increase due to contact with air [43]. Obviously, water + air mixtures rather then the liquid–gas coexistence of pure water should be considered in order to elucidate the origin of the nanobubbles.

The experimentally observed attraction between hydrophobic surfaces in liquid water [44] could be related both to the shift of the phase transition due to the confinement and (or) to the peculiarities of the water density distribution near the hydrophobic surface. In equilibrium with a bulk reservoir, a fluid confined between walls exists as a vapour (capillary evaporation) or as a liquid (capillary condensation), depending on the strength of fluid–wall interaction, bulk state and distance H between the walls [45]. In particular, the phenomenon of capillary evaporation corresponds to the equilibrium between a bulk liquid and confined vapour. Capillary evaporation was obtained in computer simulations of both LJ fluids [46–48] and water [49–51]. The phase state of a confined fluid in equilibrium with the bulk liquid under its equilibrium vapour pressure [47, 49] depends on the strength of the fluid–wall interaction only, and, in particular, for weakly attractive walls only the vapour phase is stable for any distances H between the confining (infinite) walls. In the case of an oversaturated bulk the capillary evaporation takes place at some critical distance H_{crit} between the walls [46, 48, 51], which depends on the magnitude of the applied bulk pressure. A simple estimation of the oversaturation of water at ambient conditions [7], based on the Kelvin equation, predicts a value H_{crit} of about 1000 Å. At $H < H_{\mathrm{crit}}$ the metastable liquid approaches a liquid spinodal with decreasing H, that could produce long-range attractive forces between the walls [46, 52]. Another explanation of the hydrophobic attraction is based solely on the depletion of liquid density near the solvophobic surface, and this effect was studied for fluids between hard walls [53].

The hydrophobic attraction presented above is only one of the phenomena that could be fully understood only based on the knowledge of the surface phase behaviour of fluids. This includes, in particular, the location of phase transitions and knowledge of the density distribution near the surface in various thermodynamic states. In computer simulations, surface phase diagrams have to be studied in slitlike pores, as periodic boundary conditions are not applicable to semi-infinite system. However, there are a limited number of simulated or experimentally determined coexistence curves of fluids in confinement (see [29] for a brief review and some recent studies [54–56]).

In this paper we present coexistence curves of water in hydrophobic pores of various sizes and shapes. The main goal of the present paper is studying the temperature dependence of the density profiles of a fluid near a weakly attractive surface along the liquid–vapour coexistence curve and in supercritical states of the confined fluid. The obtained results are used for the analysis of the surface critical behaviour and possible surface phase transitions. Dimensional crossover in pores and extrapolation of the observed surface critical behaviour to semi-infinite systems are discussed.

2. Method

TIP4P water [57] was simulated in slitlike pores with width H from 6 to 50 Å and in cylindrical pores with radius R from 12 to 35 Å. A spherical cutoff of 12 Å (oxygen–oxygen distance) for both the Coulombic and LJ parts of the water–water interaction potential was used. In accordance with the original parametrization of the TIP4P model, no long-range corrections were included. The interaction between the water molecules and the surface was described by a (9-3) LJ potential:

$$U_{\mathrm{w-s}}(r) = \epsilon[(\sigma/r)^9 - (\sigma/r)^3], \tag{3}$$

where r is the distance from the water oxygen to the pore wall. The parameter σ was fixed at 2.5 Å; the parameter $\epsilon = 1$ kcal mol^{-1} (producing a well-depth U_0 of the potential (3) of -0.385 kcal mol^{-1}) corresponds to a paraffin-like hydrophobic surface. Note that the (9-3) LJ potential with $\sigma = 2.5$ Å results from the integration over a flat substrate and uniformly distributed (12-6) LJ centres with $\sigma = 3.5$ Å. Numerical integrations over (12-6) LJ centres surrounding a cylindrical pore show that the value of σ remains practically the same as for the flat substrate, whereas the well-depth U_0 increases by a factor of about 1.4 and 1.2 in cylindrical pores with radii $R = 12$ and 25 Å, respectively (see [49] for the similar estimates for spherical pores). The average water density in the pore was calculated, assuming that the water occupies a pore volume until the distance $\sigma/2 = 1.25$ Å from the pore wall. Coexistence curves of water in pores in a wide temperature range were obtained by Monte Carlo simulations in the Gibbs ensemble [58]. For the three largest pores ($H = 50$ Å, $R = 30$ and 35 Å) the densities of the coexisting phases were obtained only for two temperatures (300 and 520 K). The number of successful transfers per molecule between the coexisting phases varied from 5 to about 100 in the largest and smallest pores, respectively. The number of water molecules in the two simulation cells varied from about 400 in the smallest pores up to 8000 in the largest cylindrical pore with $R = 35$ Å. The ratio L/H for slitlike pores or ratio $L/2R$ for cylindrical pores, where L is the longitudinal size of the simulation cell, always exceeded 1, and at high temperatures achieved the value 10 in the smallest slitlike pores. The density profiles of the coexisting liquid and vapour phases and in some supercritical states were obtained by subsequent Monte Carlo simulations in the NVT ensemble.

3. Results

The simulated coexistence curves of water in hydrophobic slitlike pores of various sizes are shown in figure 1. The liquid density of confined water is considerably lower then in the bulk in all the studied temperature intervals. The lowering of the pore critical temperature and the apparent flattening of the top of the coexistence curves with decreasing pore size (from $H = 30$ to 6 Å) is noticeable. A similar decrease of the liquid water density is observed in hydrophobic cylindrical pores with radii $R = 12$, 15, 20 Å [29] and $R = 25$ Å (figure 2). Note that in the case of cylindrical pores at some temperature (about 460–470 K for the pore with $R = 25$ Å)

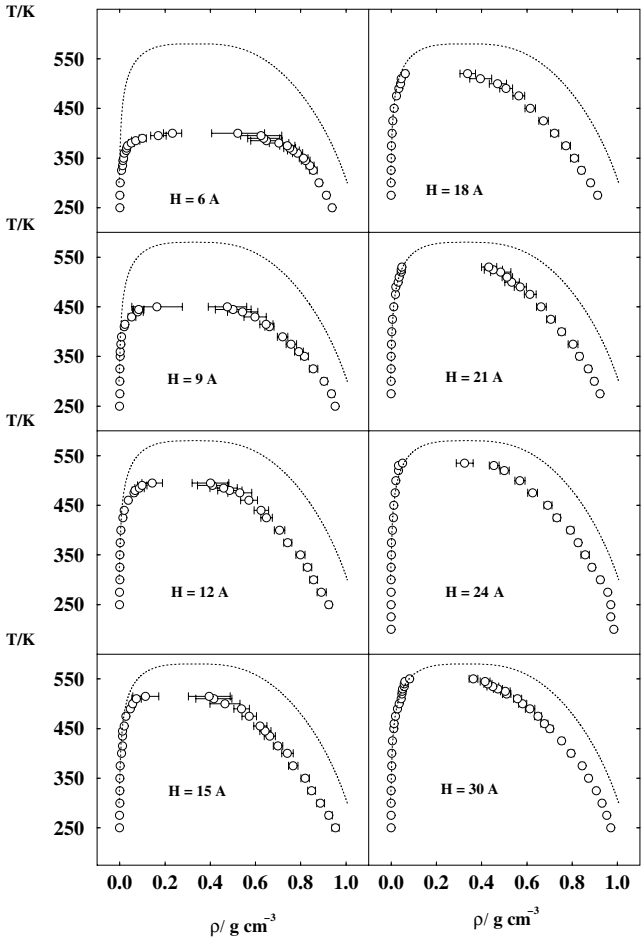

Figure 1. Liquid–vapour coexistence curves of water in slitlike hydrophobic pores. The bulk coexistence curve is shown by the dotted curve.

the decrease of the liquid density becomes more pronounced, producing a noticeable change of the slope of the coexistence curve diameter (see figure 2). In total 12 coexistence curves of water in hydrophobic pores—8 slit-like pores (figure 1) and 4 cylindrical pores (figure 2 and figure 12 of [29])—were used in this paper for the analysis of various properties of the coexisting phases of confined water.

We have estimated the pore critical temperature $T_{\mathrm{C}}^{\mathrm{pore}}$ of water in various pores as an average of two temperatures: the highest temperature, where two-phase coexistence was obtained, and the lowest temperature, where the two phases become identical in the Gibbs ensemble MC simulations (see [29] for details). The estimated values of $T_{\mathrm{C}}^{\mathrm{pore}}$ are presented in table 1. The largest uncertainty of $T_{\mathrm{C}}^{\mathrm{pore}}$ is given for narrow cylindrical pores, because the decrease of the sizes of the liquid and vapour domains with increasing temperature prevents an accurate location of the two-phase region (see [29] for a discussion of phase transitions in cylindrical geometry). Additionally, we show in table 1 the critical temperature $T_{3\mathrm{D}}$ of bulk TIP4P water and the critical temperature $T_{2\mathrm{D}}$ of quasi-two-dimensional TIP4P water with water oxygens located in one plane [29]. The evolution of the pore critical temperature $T_{\mathrm{C}}^{\mathrm{pore}}$

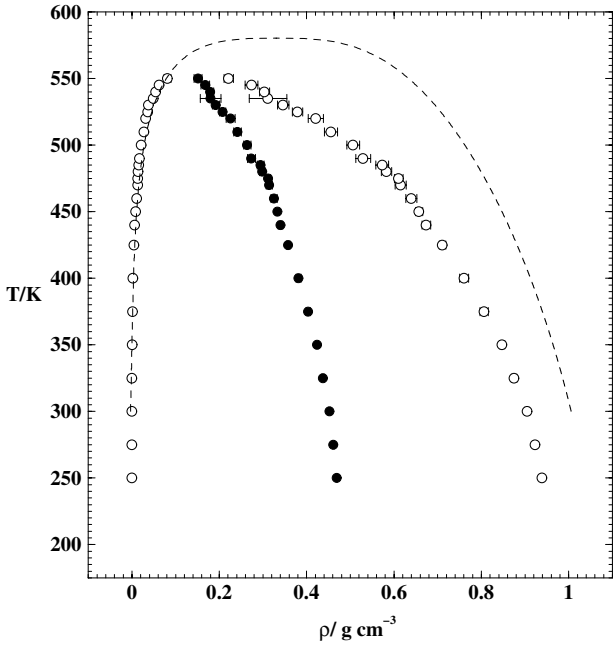

Figure 2. Liquid–vapour coexistence curve of water in the cylindrical hydrophobic pore with $R = 25$ Å. The diameter of the coexistence curve is shown by closed circles. The bulk coexistence curve is shown by the dashed curve.

Table 1. Estimated pore critical temperature T_C^{pore} (in K) and pore critical density ρ_C^{pore} (in g cm^{-3}) of TIP4P water in hydrophobic pores.

Pore width (Å)	T_C^{pore}	ρ_C^{pore}
	Cylindrical pores	
$R = 12$	535.0 ± 15.0	0.220 ± 0.007
$R = 15$	535.0 ± 10.0	0.172 ± 0.007
$R = 20$	540.0 ± 5.0	0.156 ± 0.007
$R = 25$	555.0 ± 5.0	0.150 ± 0.007
	Slitlike pores	
Quasi-2D water	330.0 ± 7.5	
$H = 6$	402.5 ± 2.5	0.358 ± 0.007
$H = 9$	452.5 ± 2.5	0.294 ± 0.007
$H = 12$	497.5 ± 2.5	0.262 ± 0.007
$H = 15$	520.0 ± 5.0	0.246 ± 0.007
$H = 18$	525.0 ± 5.0	0.235 ± 0.007
$H = 21$	535.0 ± 5.0	0.241 ± 0.007
$H = 24$	540.0 ± 5.0	0.229 ± 0.007
$H = 30$	555.0 ± 5.0	0.227 ± 0.007
bulk 3D water	580.2 ± 2.5	0.330 ± 0.003

with pore size is shown in figure 3. The shift of the critical temperature in slitlike pores was fitted to the power law

$$\Delta T_C = (T_{3D} - T_C^{pore})/T_{3D} \sim (\Delta H)^{-\theta}. \tag{4}$$

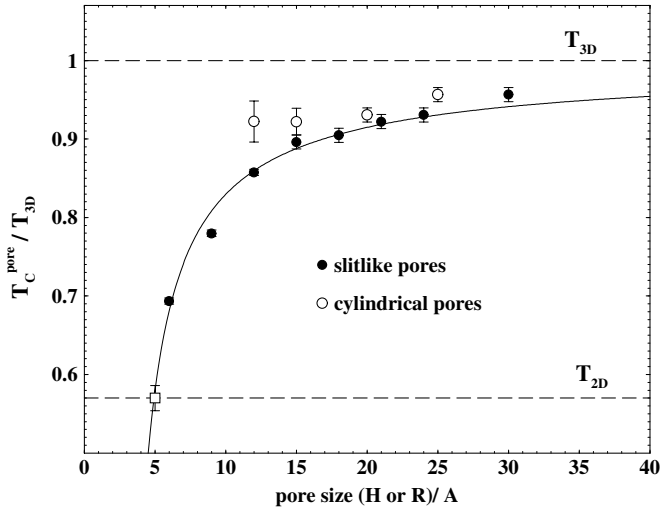

Figure 3. The dependence of the pore critical temperature on the pore size. Closed symbols—slitlike pores. Open symbols—cylindrical pores. The critical temperatures of bulk and quasi-two-dimensional water are shown by dashed lines. The square corresponds to the critical temperature of the quasi-two-dimensional water, attributed to $H = 5$ Å. The solid curve is a fit of equation (4) to the data for slitlike pores (see the text for details).

In the limit of a thick fluid film, the value of θ is expected to be equal to $\theta = 1/\nu_{3D}$ ($\nu_{3D} = 0.63$ [18]) from finite-size scaling arguments [61]. For a thin film the effective value of θ should be equal to 1 [30, 62]. The thickness of the fluid film ΔH in a slitlike pore is lower than the pore width H by $\sigma = 2.5$ Å, the LJ parameter for the water–substrate interaction. We attributed quasi-two-dimensional water to water in a pore with effective size $H = 5$ Å, that approximately corresponds to a water monolayer, strongly localized in one plane.

A fit of equation (4) to the data for slitlike pores (the solid curve in figure 3) gives the value $\theta = 0.82$. However, a plot of ΔT_C versus ΔH in double logarithmic scale (figure 4) shows that most of the data points may be well fitted by a linear law ($\theta = 1$), whereas the largest pore studied ($H = 30$ Å) shows a trend toward $\theta = 1/0.63$. This suggests a crossover between two kinds of behaviour at a pore size $H = 24$ Å, that corresponds to a film of width roughly 8 molecular diameters. Note that the data points both for the narrowest pore ($H = 6$ Å) and quasi-two-dimensional water bend down from the linear dependence (figure 4).

A polynomial extrapolation of the diameter of the coexistence curves $\rho_d = (\rho_l + \rho_v)/2$ to the pore critical temperature was used to estimate the pore critical densities ρ_C^{pore}, presented in table 1. In all pores, excluding the smallest one, the pore critical density is considerably below the bulk value $\rho_{3D} = 0.330$ g cm^{-3} [29]. Moreover, in the considered range of pore sizes (up to $H = 30$ Å) ρ_C^{pore} decreases with increasing pore size and shows no tendency towards the bulk critical value (figure 5).

In order to understand the observed peculiarities of the coexistence curves and to study the surface critical behaviour of water in hydrophobic pores, we analysed the density profiles of the coexisting phases and their evolution with temperature. Typical density profiles of water in the liquid and vapour phases are shown in figures 6 and 7, respectively. The density of the liquid phase is strongly depleted towards the pore wall, and this depletion progressively intensifies with temperature (figure 6) and pore size. This effect is noticeably stronger in cylindrical pores in comparison with slitlike pores. Note that the depletion of the density is accompanied by an essential increase of diffusivity near the hydrophobic surface [63].

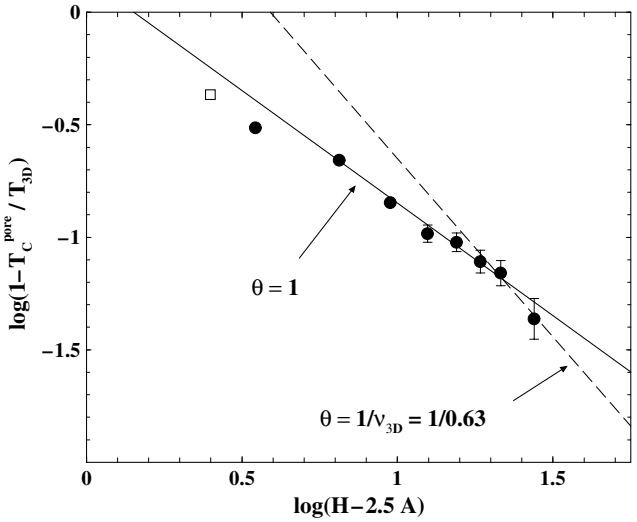

Figure 4. The dependence of the pore critical temperature on the size of the slitlike pore in double logarithmic scale. The square corresponds to the critical temperature of the quasi-two-dimensional water, attributed to $H = 5$ Å.

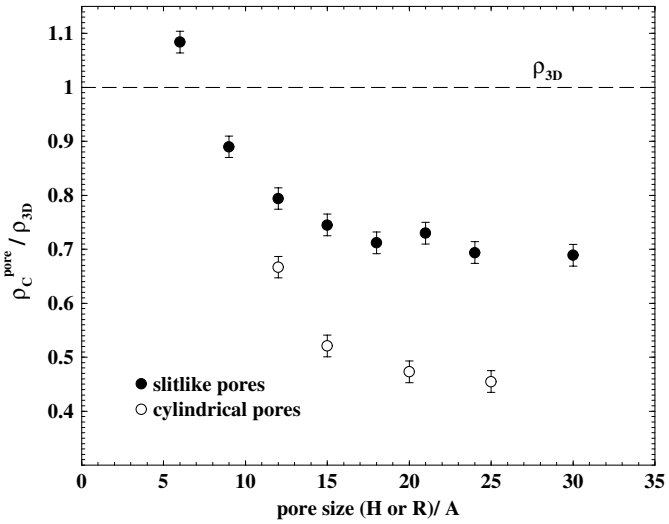

Figure 5. The dependence of the pore critical density, normalized to the bulk critical density, on the pore size. Closed symbols—slitlike pores. Open symbols—cylindrical pores. The critical density of bulk water is shown by the dashed line.

The density profiles in the vapour phase show preferential adsorption of the water molecules at weakly attractive wall at temperatures below ≈500 K. At higher temperatures the vapour phase shows a depletion of the density towards the pore wall, similar to the liquid phase (figure 7). This means that at $T < 500$ K the density profile of the liquid bends downwards, whereas the density profile of the vapour bends upwards when approaching the pore wall. A similar behaviour was observed in lattice gas simulations at temperatures below the wetting transition [64] and in MC simulations of LJ fluids near a weakly attractive substrate, including temperatures close to the critical temperature [65].

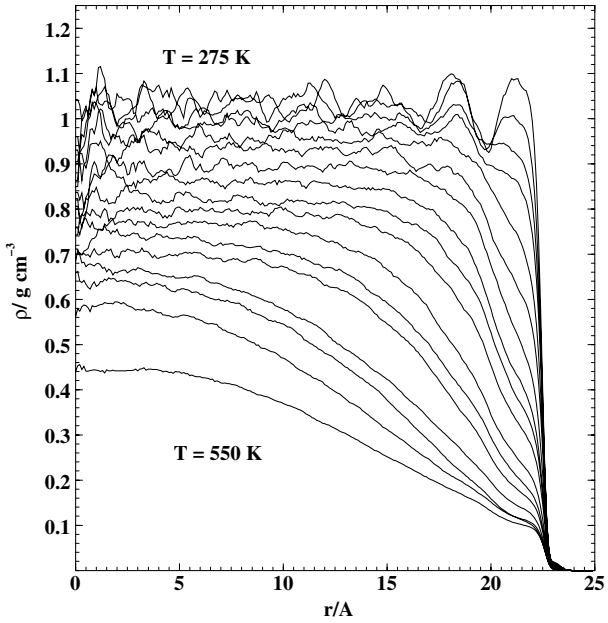

Figure 6. Density profiles of water in the liquid phase along the coexistence curve in the cylindrical pore with $R = 25$ Å.

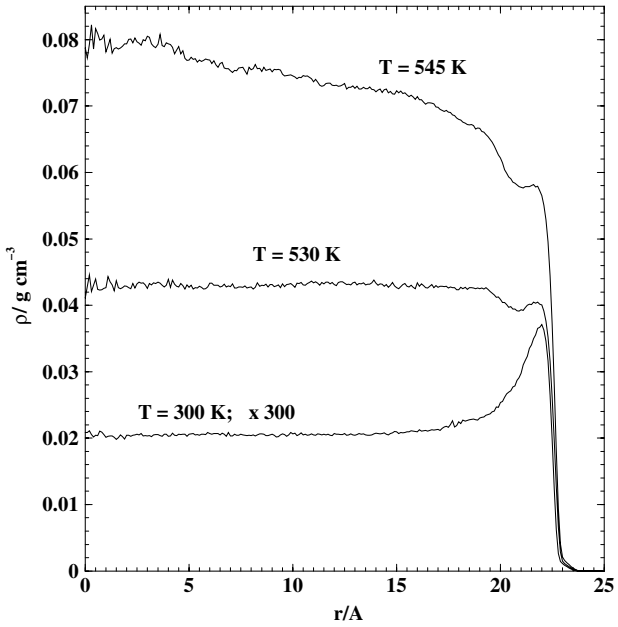

Figure 7. Density profiles of the water vapour phase along the coexistence curve in the cylindrical pore with $R = 25$ Å. For 300 K the density is multiplied by the factor 300.

Due to the spatial heterogeneity of fluids in pores the local coexistence curves, i.e. the temperature dependence of the densities of the coexisting phases at various distances from the

surface, should be analysed. Defining layers (and, first of all, the surface layer) in continuous models, which allows a direct comparison with the results for lattice models, is not clear *a priori*. Far from the surface, where the packing of the fluid molecules at the surface is negligible and the density varies smoothly, the layer thickness could be arbitrarily small. Near the surface, both the packing effect and the details of the fluid–surface interaction become important. Therefore, it seems reasonable to consider the local densities ρ_i, averaged over layers of thickness one molecular diameter. The location of the first (surface) layer was chosen between the first minimum in the liquid density distribution at low temperatures (typically about 5 Å from the pore wall) and the van der Waals water–wall contact ($\sigma/2 = 1.25$ Å from the wall). The thickness of the subsequent water layers was set to 3 Å. The average density of the 'inner' water near the pore centre was calculated for a layer extending 4–8 Å from the pore centre. The coexistence curves of water in the surface layer and of water in the pore interior for some cylindrical and slitlike pores are shown in figure 8. While the coexistence curve of 'inner' water (figure 8(b)) is close to the bulk one (except for the proximity of the pore critical temperature), the surface water shows a drastically different behaviour (figure 8(a)). The density of the liquid phase in the surface layer approaches extremely low values (considerably below ρ_{3D}) with increasing temperature, and the coexistence curve shows triangularlike shape. Note the highly universal behaviour of the 'inner' water and the rather similar behaviour of the surface water in the pores of various sizes and shapes.

The analysis of the shape of the coexistence curves in fluid systems includes the temperature dependence of the order parameter and diameter. Because of the zero critical magnetization of an Ising system, its order parameter is simply the magnetization (bulk or local). In confined fluids (as well as in the bulk) the critical density ρ_C is non-zero, and in the asymptotic limit the order parameter is the deviation of the densities ρ_l and ρ_v of the coexisting liquid and vapour phases from ρ_C. Apart from the critical point, the temperature dependence of the diameter $\rho_d = (\rho_l + \rho_v)/2$ should be taken into account and so the order parameter is defined as the deviation of the density from the diameter $\Delta\rho = (\rho_l - \rho_v)/2$. We define the local order parameter of a fluid in a similar way: $\Delta\rho(z) = (\rho_l(z) - \rho_v(z))/2$, where the densities of liquid and vapour are taken at the same distance z from the surface. The temperature dependence of the bulk order parameter near the critical point in magnets, as well as in fluids, obeys the simple scaling law

$$\Delta\rho \sim \tau^{\beta}, \tag{5}$$

where $\tau = (T_{3D} - T)/T_{3D}$ is a reduced temperature and $\beta = 0.326$ [18] is a universal critical exponent of 3D (bulk) systems. The local order parameter $\Delta\rho(z)$ should obey the same law, but with another critical exponent, which depends on the surface universality class. The temperature dependence of the local order parameter $\Delta\rho_i$ for surface water, inner water and two intermediate water layers is shown in figure 9 in double logarithmic scale. The slope of these curves is equal to the exponent β of the power law, equation (5). The order parameter of 'inner' water follows closely the bulk behaviour up to $\tau = 0.08$. The order parameter in the surface layer shows an essentially different behaviour: starting from extremely low temperatures $\tau = 0.57$ (close to freezing temperature $\tau = 0.59$ of TIP4P bulk water [66]) the order parameter follows the scaling law with a value of the exponent β close to the value $\beta_1 = 0.82$ of the ordinary transition in the Ising magnets. The intermediate two layers show a crossover from bulk-like behaviour to surface behaviour at $\tau = 0.22$ and 0.11, in the second and the third layers, respectively. A higher value of the exponent β in the surface layer means that the densities of the coexisting phases near the surface approach each other much faster with temperature than in the pore interior.

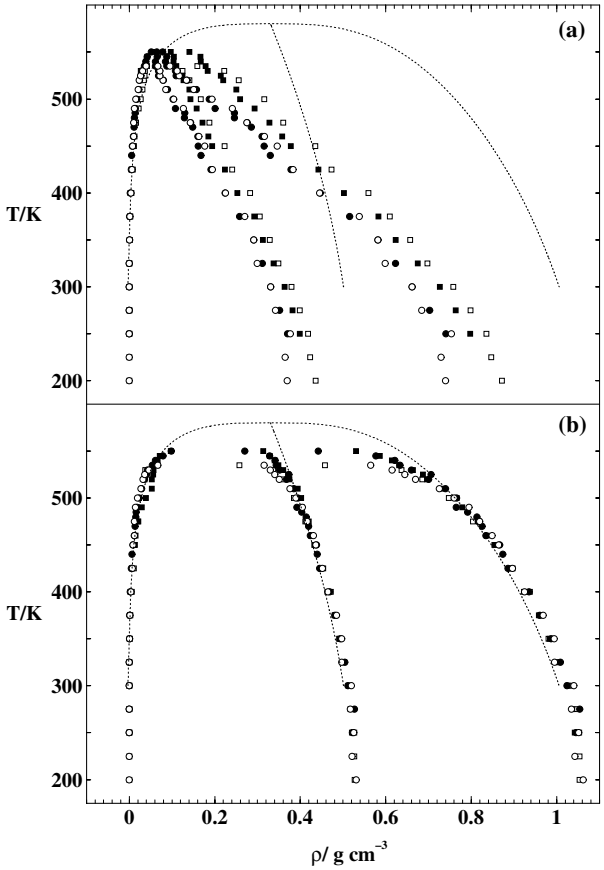

Figure 8. Coexistence curves and diameters of water in hydrophobic pores: closed circles—cylindrical pore with $R = 25$ Å; open circles—cylindrical pore with $R = 20$ Å; closed squares—slitlike pore with $H = 30$ Å; open squares—slitlike pore with $H = 24$ Å. (a) Water in the surface layer; (b) water in the pore interior. The coexistence curve and diameter of bulk TIP4P water are shown by dotted curves.

This disordering effect of the surface may also be illustrated, using an effective exponent β^{eff}, defined as

$$\beta^{\text{eff}}(z, \tau) = \mathrm{d}\ln(\Delta\rho(z, \tau))/\,\mathrm{d}\ln\tau. \tag{6}$$

The value of the exponent β^{eff} is close to the value of some true critical exponent in the temperature intervals, which are outside the crossover regions. $\beta^{\text{eff}}(z)$, obtained by applying equation (6) to $\Delta\rho(z, \tau)$ for the interval $\tau \leqslant 0.31$, is shown in figure 10 as a function of the distance to the pore centre. In fact, the value β^{eff} is close to the 3D Ising value in the pore interior, and varies between 0.8 and 1.0 in the surface layer (the hatched area in figure 10). Note that the maximum of β^{eff} corresponds to the minimum of the LJ water–wall potential, which causes a slight hump of the liquid density profile (see figure 10).

The behaviour of the order parameter in the surface layer is rather universal in the three largest slitlike pores, and is close to the simple power law with β_1 of about 0.8 (figure 11(a)). In the pores with $H < 21$ Å the dependence $\ln(\Delta\rho_1)$ versus $\ln(\tau)$ progressively bends down at high temperatures (figure 11(b)), preventing the location of a proper temperature interval, where the simple power law is valid.

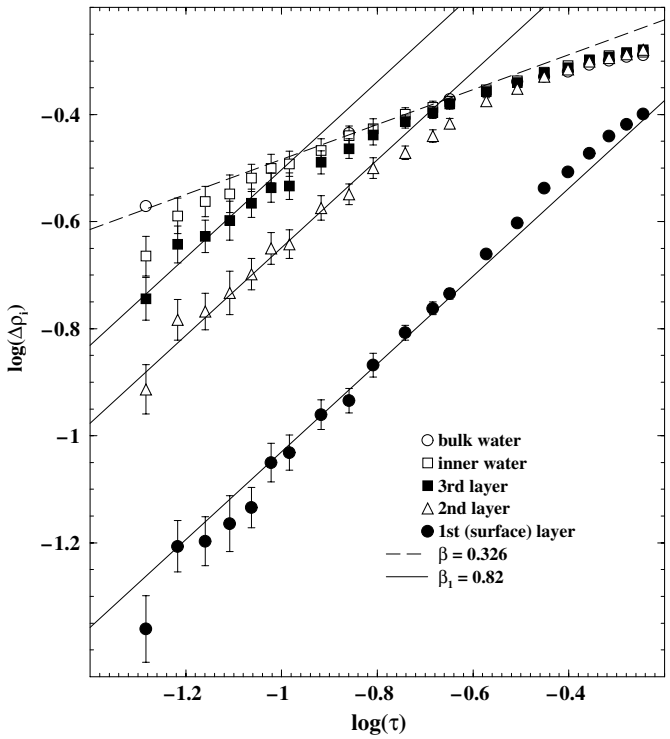

Figure 9. The variation of the local order parameter $\Delta\rho_i$ with reduced temperature τ in the slitlike pore with $H = 30$ Å (double logarithmic scale).

Whereas the behaviour of water in the surface layer of cylindrical pores in general looks rather similar to that in slitlike pores (figure 8(a)), the variation of the local order parameter $\Delta\rho_1$ with reduced temperature shows serious differences (the full circles in figure 12). $\Delta\rho_1$ follows roughly the simple power law with $\beta_1 \sim 0.8$ at $\tau \geqslant 0.20$, whereas at higher temperatures a simple power law with another exponent of β_1 of about 1.8 is observed (figure 12). In the second and subsequent layers, the behaviour with the exponent $\beta_1 \sim 0.8$ could not be detected, but an apparent crossover from the bulk-like behaviour ($\beta \sim 0.326$) at low temperatures to the behaviour with β_1 of about 1.8 could be seen. In the second layer the bulk-like behaviour is observed up to $\tau \sim 0.18$, whereas the behaviour with β_1 of about 1.8 is valid at $\tau \leqslant 0.11$. In the subsequent layers this crossover region becomes narrower and shifts to higher temperatures.

4. Discussion

The presented coexistence curves and density profiles give us the possibility to verify theoretical predictions of confinement effects. Additionally, they give us the possibility to study phase transitions near single surfaces by extrapolating the pore results to semi-infinite systems.

The observed evolution of the pore critical temperature with the size of the slitlike pores is in general agreement with theoretical predictions and simulations for the 3D Ising model. In particular, the shift of the critical temperature in the pores which contain from 2 to 7 molecular layers is inversely proportional to the pore size (see figure 4 and equation (4)), while in the largest pore studied (9 molecular layers) a crossover to a power law dependence with $\theta = 1/\nu_{3D}$ is indicated. In Ising films such a crossover begins when their thickness achieves 4–8 layers [67–70]. The critical temperatures of quasi-two-dimensional water and

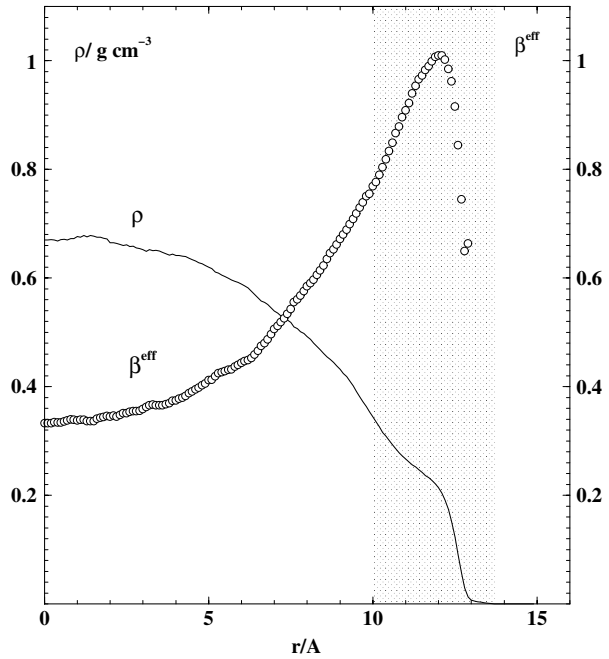

Figure 10. The variation of the effective exponent β^{eff}, obtained by applying equation (6) to the local order parameter $\Delta\rho(z, \tau)$, with approaching pore wall in the slitlike pore with $H = 30$ Å (circles). The liquid density profile at $T = 400$ K is shown by a curve. The hatched area indicates the location of the first (surface) water layer.

water in a pore, comprising a single water layer ($H = 6$ Å), deviate from the main dependence $\Delta T_{\text{C}} \sim \Delta H^{-1}$. This deviation is in agreement with the behaviour of a monolayer Ising film [67–70]. Obviously, with the decrease of the pore width from 2 to 1 monolayer, the system loses any features of three-dimensionality and becomes essentially two-dimensional.

The dimensional crossover from 3D critical behaviour to 2D behaviour in slitlike pores is expected at temperatures where the correlation length becomes comparable with the pore size. It appears particularly as a change of the critical exponent of the order parameter in the power law, equation (5), where $\tau_{\text{pore}} = (T_{\text{C}}^{\text{pore}} - T)/T_{\text{C}}^{\text{pore}}$ is used instead of τ. The average order parameter (i.e., the difference of the densities, which are averaged over the whole pore) should be used here. In the four largest pores a crossover to the 2D behaviour is seen (figure 13, left-hand panel), when the correlation length exceeds about 15% of the pore width (estimates of the correlation length are given below).

A quite different behaviour of the order parameter is observed for essentially two-dimensional phase transitions, i.e. for the liquid–vapour phase transition of water in the smallest studied hydrophobic slitlike pore ($H = 6$ Å, monolayer width) and for the layering transition of water at a hydrophilic substrate (slitlike pore with $H = 24$ Å and $U_0 = -4.62$ kcal mol^{-1}, [29]). In both cases the centres of water molecules are located in a layer of about 1–2 Å width, the critical temperatures of both transitions are close (400 ± 5 K), and the order parameter follows a power law with the 2D exponent $\beta = 0.125$ in the low temperature region (figure 13, right-hand panel). When the temperature exceeds about 375–385 K ($\tau_{\text{pore}} \approx 0.04$–$0.06$) the behaviour of the order parameter in these systems indicates a crossover to a mean-field behaviour with exponent $\beta = 0.5$. Such a crossover is expected when

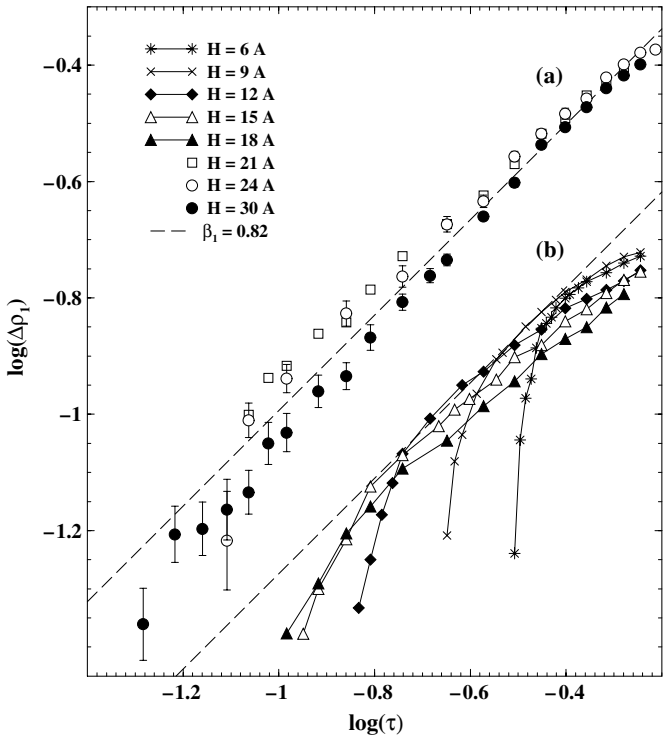

Figure 11. A double logarithmic plot of the local order parameter in the surface layer $\Delta\rho_1$ versus reduced temperature τ in *slitlike* pores. (For the two narrowest pores all molecules were attributed to the surface layer.) The data points for the pores with $H \leqslant 18$ Å are shifted by -0.40 (curves b).

the correlation length becomes comparable to the lateral size L of the simulation cell [71, 72]. In these 'one-layer systems' the phase transition is essentially two-dimensional, and so the 2D correlation length diverges at their critical temperatures. A rough estimate with $\nu_{2D} = 1$ and the 3D bulk value of the amplitude ξ_0 [73] shows a crossover to the mean-field behaviour when the 2D correlation length has grown to about 15–20% of L. The lateral system size used for the simulations of a layering transition [29] is about 50% larger than in the case of the hydrophobic pore with $H = 6$ Å. This causes a larger finite-size effect in the latter case. Note that a variation of the critical temperature within the interval estimated from GEMC (see table 1) does not restore the asymptotic 2D behaviour in the hydrophobic pore.

In the pores of intermediate sizes ($H = 9$, 12 and 15 Å, i.e. from 2 to 4 molecular layers' width) we cannot observe any tendency to the 2D behaviour, contrary to the expectation that the region of 2D behaviour should be considerably wider than in larger pores. This cannot be the result of a crossover to a mean-field behaviour due to finite L, as in the case of quasi-two-dimensional systems considered above. In the two largest pores ($H = 24$ and 30 Å), where the lateral size L is about twice the pore size H, the trend to mean-field behaviour is noticeable for the highest temperature point only. In smaller pores the ratio L/H is larger, from 3 to 10, and therefore no trend to mean-field behaviour should be expected even at higher temperatures than in the largest pores. The apparent 3D Ising behaviour in a wide temperature interval, observed in pores of 2–4 molecular layer width (figure 13, $H = 9$–15 Å), could be the result of a competition between the trend towards 2D criticality and a progressive contribution to the order parameter from the surface layers, which show faster disordering compared to the

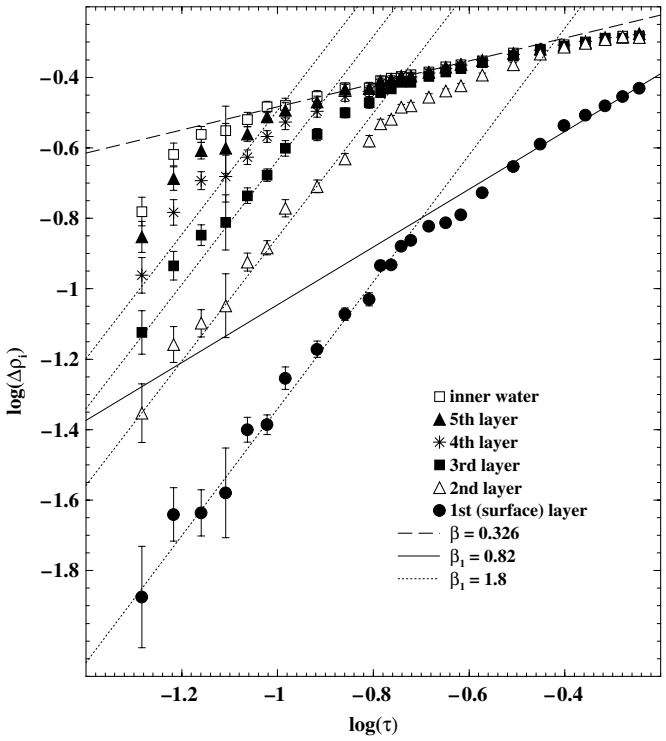

Figure 12. The variation of the local order parameter $\Delta\rho_i$ with reduced temperature τ in a *cylindrical* pore with $R = 25$ Å in double logarithmic scale.

bulk. Dimensional crossover in small pores certainly needs further studies both for fluid and lattice [70] systems.

The common feature of the coexistence curves of water in all 12 hydrophobic pores studied is a significant decrease of the density at the liquid branch in comparison with the bulk (see figures 1, 2 and also figure 12 in [29]). An inspection of the density profiles evidences that this decrease is due to the lowering of the density near the pore wall (figure 6), which appears as a gradual decline of the water density towards the surface without any evidence for the formation of a vapour layer. This agrees with the recent experimental studies of water density depletion near hydrophobic surfaces at ambient [37–40] and elevated [40, 74] temperatures. The absence of a vapour layer near the hydrophobic surface means the absence of drying (or predrying) transitions at $T < T_C$. This agrees with expectations from theory, concerning the phase behaviour near a surface with long-range fluid–surface interaction [11, 12], and is confirmed by computer simulations of LJ fluids near weakly attractive walls [65]. Our simulations of water near an extremely hydrophobic surface (less attractive than a paraffin-like surface) suggest that a stable vapour layer could never occur near a real hydrophobic surface, which always interacts with water via attractive long-range van der Waals forces. The possible existence of a metastable vapour layer near a hydrophobic surface deserves further investigations.

Due to the absence of a surface transition, a study of the surface critical behaviour of the fluid becomes possible. The obtained density profiles of the coexisting phases at various temperatures allow us to study the temperature dependence of the order parameters in various layers. In the large slitlike pores the order parameter in the surface layer $\Delta\rho_1(\tau)$ demonstrates a universal temperature dependence, consistent with the exponent $\beta_1 = 0.82$ of the ordinary

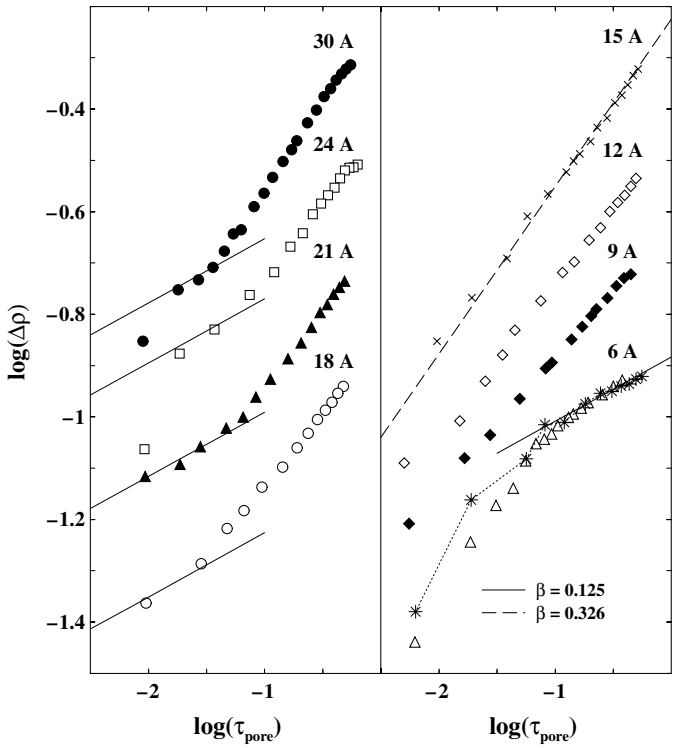

Figure 13. The variation of the order parameter $\Delta\rho$ from pore averaged densities with reduced temperature τ_{pore} in slitlike hydrophobic pores (double logarithmic scale). The pore widths H are indicated in the figure. The data points are shifted progressively by -0.20. The data points for the layering transition are shown by stars (see the text for details).

transition (figure 11(a)). In the second and subsequent layers, $\Delta\rho_i(\tau)$ shows a crossover from bulk to surface critical behaviour with increasing temperature (figure 9). The increase of the crossover temperature with the distance to the surface agrees with the expectation that intrusion of the surface perturbation into the bulk is governed by the bulk correlation length [14]. As a result, the effective critical exponent β^{eff} varies smoothly from the bulk value in the pore interior to the value β_1 near the surface (figure 10). A very similar crossover behaviour was observed for the ordinary transition in Ising magnets [75–78].

Figure 11 shows that in the three largest slitlike pores a power law with exponent $\beta_1 \approx 0.8$ is valid for the surface layer in an extremely wide temperature range (about 250 K). This means that the surface behaviour in these pores is close to that in semi-infinite systems, and the influence of the opposite wall is negligible up to a few degrees from $T_{\text{C}}^{\text{pore}}$. In smaller pores the effective value of β_1 shows a rapid increase when approaching $T_{\text{C}}^{\text{pore}}$. This effect is more pronounced and starts at lower temperatures in narrower pores. This evidences the influence of the opposite wall on the surface critical behaviour.

In cylindrical pores the temperature evolution of the order parameter is in general similar to that in slitlike pores. Namely, the effective critical exponent β^{eff} increases when approaching the surface, and achieves values which are considerably higher than the bulk critical exponent (figure 12, see also figure 5 in [28]). However, in contrast to the planar surface, the critical behaviour of the order parameter in the surface layer even in large pores shows a sharp temperature crossover from the exponent $\beta_1 \approx 0.8$ to a much higher value (figure 12). This

effect is so strong that it can be seen as a pronounced shoulder on the liquid branch and diameter of the coexistence curve of water in the pores with radius $R = 25$ Å (figure 2), $R = 15$ and 20 Å (figure 12 in [29]). This shoulder seems to shift to higher temperature with increasing pore radius. The order parameter in the second and subsequent layers does not show a behaviour with an exponent $\beta_1 \approx 0.8$, rather a crossover directly from the bulk-like behaviour to the behaviour with $\beta_1 \approx 1.8$ occurs (figure 12). This phenomenon is obviously caused by the deviation of the surface from planarity. The critical behaviour of the order parameter near cylindrical surfaces has not yet been studied. Our results suggest that a power law critical behaviour could also be valid for such geometries. The obtained value of $\beta_1 \approx 1.8$ is comparable with the value 1.86 for the corner magnetization of a cube, and to values observed for edges with an opening angle less than $\pi/2$ [32].

The local order parameter $\Delta\rho(z, \tau)$, used in the present paper, was defined similarly as for the bulk fluid (see above). Like in the bulk case, the order parameter is the deviation of the density from the diameter. In the fluid near the surface the diameter depends not only on temperature, but also on the distance from the surface. Such a definition of $\Delta\rho(z, \tau)$ provides a vanishing local order parameter at the critical point at any distance from the surface, i.e. the profile of the order parameter is flat ($\Delta\rho(z, \tau = 0) \equiv 0$), exactly as in the case of the ordinary transition of Ising magnets [14]. In large pores the temperature dependence of the diameter of the coexistence curve in the pore interior is close to the bulk behaviour up to the temperature where the 'inner' water is influenced by the surface (figure 14). In the surface layer the local diameter ρ_d shows a perfect linear temperature dependence over the whole temperature range (figure 14). The critical density in the surface layer decreases with increasing pore size and achieves an extremely low value (0.06 g cm^{-3} in a slitlike pore with $H = 30$ Å). This results in a decrease of the average pore critical density with increasing pore size (figure 5) and may indicate a drying transition at the critical point of a semi-infinite system.

The profiles of $\Delta\rho(z, \tau)$ could provide additional information concerning the surface critical behaviour of fluids. The profile of magnetization was studied in mean-field approximation for both the ordinary and extraordinary transitions [79]. In the case of an ordinary transition ($h_1 = 0$), the local magnetization is symmetrical in the two phases and therefore serves as order parameter. Near the surface it obeys the following dependence on the distance z to the surface [14, 59, 60]:

$$\Delta\rho(z) = \Delta\rho_{\text{bulk}} \tanh(z/(2\xi_-) + z^*), \tag{7}$$

where $\Delta\rho_{\text{bulk}}$, the value of the bulk order parameter, and ξ_-, the bulk correlation length ($T < T_C$), depend only on temperature, while z^* is connected with the density profile close to the surface and is determined by the surface–fluid interaction (in an Ising system it is directly related to the so-called extrapolation length λ). The distance $z = 0$ was assigned to 1.25 Å from the wall, which corresponds to the boundary of the volume occupied by water (see section 2). In [79] another equation was proposed:

$$\Delta\rho(z) = \Delta\rho_{\text{bulk}} \frac{\sqrt{1 + (\lambda/\xi_-)^2} - 1 + (\lambda/\xi_-)\tanh(z/2\xi_-)}{(\lambda/\xi_-) + (\sqrt{1 + (\lambda/\xi_-)^2} - 1)\tanh(z/2\xi_-)}, \tag{8}$$

which reduces to equation (7) for small λ/ξ_-.

Depletion of water density near the surface could be also analysed in the framework of normal transition, assuming the preferential adsorption of voids. As the normal transition in the limit of $h_1 \to \infty$ is equivalent to the extraordinary transition [20], the preferential adsorption in mean-field approximation could be described as [59, 79]

$$\rho(z) = a_1 - a_2 \coth(z/(2\xi_-) + z^*), \qquad \text{when } T < T_C \tag{9}$$

$$\rho(z) = \rho_{\text{bulk}} + a_1/\sinh(z/\xi_+ + z^*), \qquad \text{when } T > T_C, \tag{10}$$

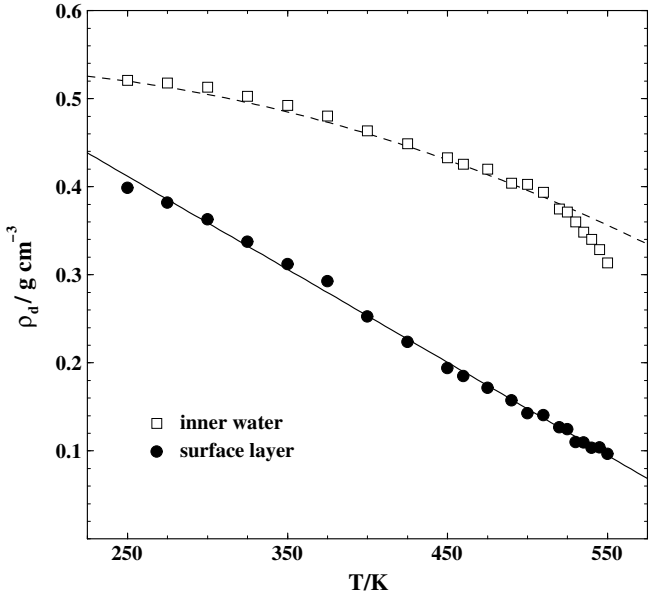

Figure 14. The temperature dependence of the diameter ρ_d for surface layer and inner water in a slitlike pore with $H = 30$ Å. The solid line is a linear fit of the diameter in the surface layer. The diameter of bulk TIP4P water [29] is shown by the dashed curve.

which provides an infinite adsorption at the distance $z = -2\xi_- z^*$ from the surface. ξ_+ is the bulk correlation length at $T > T_C$. At subcritical temperatures we fitted equation (9) to the density profiles of the coexisting phases and of the fluid order parameter $\Delta\rho$. In the latter case $\Delta\rho_{bulk} = (a_1 - a_2)$.

A renormalization group analysis of the magnetization profile at the ordinary transition of an Ising lattice shows that very close to the surface ($z \ll \xi_-$) the order parameter profiles obey a power law dependence $\Delta\rho(z) \sim z^{(\beta_1-\beta)/\nu}$, and at $z \approx \xi_-$ cross over to an exponential behaviour [14]. The deviation of the scaling behaviour from the mean-field profile (equations (7) and (8)) is noticeable in the range $0 < z < 2\xi_-$, and achieves its maximum value of about 4% at $z \approx \xi_-/2$ [80]. The presence of pronounced density oscillations of fluids near surfaces even at high temperatures makes it reasonable to neglect these small corrections and to use in our study the mean-field equations (7)–(10) to fit the order parameter and density profiles.

We have fitted the profiles of $\Delta\rho(z)$ as well as $\rho_l(z)$ and $\rho_v(z)$ separately with equations (7)–(9) and the supercritical profiles of $\rho(z)$ with equation (10), assuming all parameters to be freely variable. Equations (7) and (8) provide equally good descriptions of the order parameter profiles in all studied slitlike pores and in the whole temperature range (see figure 15, where fits using equation (7) are shown). This evidences that in our system the extrapolation length λ is negligibly small. Indeed, its value practically does not depend on temperature and varies between 0 and 0.5 Å. The order parameters $\Delta\rho_{bulk}$ obtained from fits using equations (7) and (8) are close to the order parameter in bulk water at all temperatures [29]. Small systematic deviations of the fitting curves from the order parameter in the pore interior, which are noticeable at high temperatures, are caused by deviations of $\Delta\rho$ in the pore interior from the bulk value discussed above and shown in figure 9.

The temperature dependence of ξ_- obtained from equations (7) and (8) shows reasonable agreement with the experiment (figure 16). Moreover, at $\tau < 0.15$ the correlation length shows

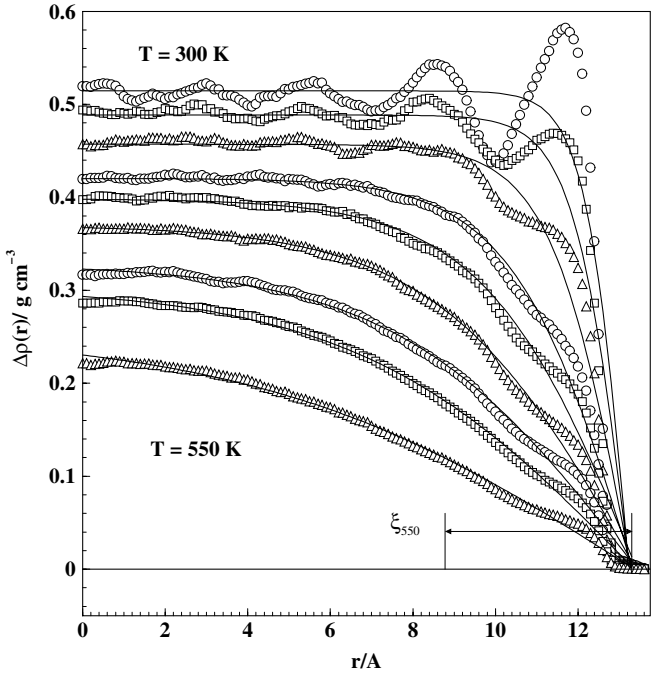

Figure 15. Fitting of the order parameter profiles $\Delta\rho(r)$ in the slitlike pore with $H = 30$ Å to equations (7) and (8) at several temperatures: $T = 550$, 535, 525, 500, 475, 450, 400, 350 and 300 K. The value of the correlation length, obtained from the fits, is shown for the highest temperature.

the expected power law behaviour $\xi_-(\tau) \sim \tau^{-\nu}$ with $\nu = \nu_{3D} = 0.63$ (figure 17). Note that the values of ξ_- were obtained for a slitlike (and not a semi-infinite) geometry and, therefore, the correlation length ξ_- increases with increasing pore size. For example, at $T = 520$ K $\xi_- = 1.76$ Å in the pore with $H = 18$ Å, whereas in the pore with $H = 50$ Å it achieves 3.14 Å, which seems to be nearly converged (see the vertical bar in figure 16) to the value of the bulk correlation length ξ_- in a semi-infinite system ($H \to \infty$). The progressive lowering of the effective ξ_- with decreasing pore size reflects the shift of the phase transition in the pore away from the bulk phase transition.

Using equations (7) and (8) to describe the order parameter profiles in cylindrical pores results in increased effective values of the correlation length. As in the case of slitlike pores, ξ_- progressively lowers with decreasing pore size. However, the absolute value of ξ_- considerably exceeds the values of ξ_- in slitlike pores of comparable sizes, especially at high temperatures. Obviously, the order parameter profiles in cylindrical and slitlike geometries should be described by different functions [81], and the critical behaviour of fluids near cylindrical surfaces deserves further study.

The fitting of equation (9) to the order parameter $\Delta\rho(z)$ is of lower quality in comparison with the fitting of equations (7) and (8). The obtained correlation lengths follow an unexpected linear temperature dependence in the double logarithmic plot of figure 17. So, the order parameter profiles $\Delta\rho(z)$ show a behaviour which is in accordance with an ordinary transition.

The density profiles in the liquid phase $\rho_l(z)$ in the whole temperature range could be fitted with the same quality by any of the equations (7)–(9). The values ξ_- obtained from the fits using equations (7) and (8) are about 70% of the values of ξ_- obtained from $\Delta\rho(z)$.

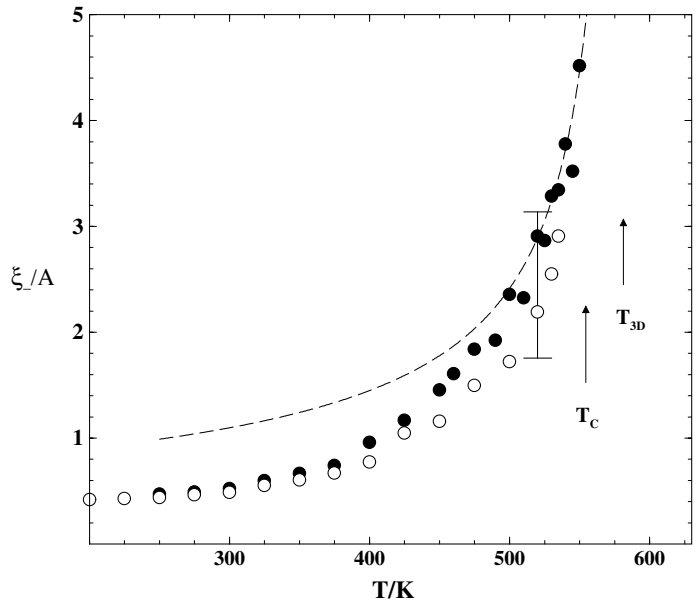

Figure 16. The temperature dependence of the effective value of the correlation length along the coexistence curve obtained by fitting equations (7) and (8) to the order parameter profiles of the slitlike pores with $H = 30$ Å (solid circles) and $H = 24$ Å (open circles). The simple scaling behaviour of the correlation length $\xi_- = \xi_0 \tau^{-0.63}$ with the experimentally obtained value $\xi_0 = 0.694$ Å [73] is shown by dashed curve. The vertical bar shows the increase of ξ_- at $T = 520$ K with increasing pore size from $H = 18$ to 50 Å.

The values of ξ_- obtained from the fits using equation (9) at low temperatures are practically equal to the values ξ_- obtained from the corresponding fits of $\Delta\rho(z)$, but deviate noticeably in the high temperature region, where the temperature dependence becomes consistent with the expected scaling law (figure 17). Values of ξ_- obtained from the fit of the vapour density profiles $\rho_v(z)$ at high temperatures are several times smaller than the values ξ_- obtained from the fits of $\rho_l(z)$ and $\Delta\rho(z)$.

The density profiles of supercritical water ($T = 580$ K) at several average densities were satisfactorily fitted by using equation (10) (see figure 18), while the quality of the fits with equation (7) was noticeably worse. The density dependence of the obtained correlation length ξ_+ shows a pronounced maximum when the average density is close to the critical density of the bulk TIP4P water $\rho \approx 0.330$ g cm^{-3} [29] (figure 19). A similar dependence was observed experimentally for supercritical water [82]; however, the absolute values of the correlation length, obtained from simulations, are considerably smaller, as they are obviously suppressed by the finite size of the simulated cells.

Summarizing our studies of the order parameter and density profiles, we conclude that:

(i) at $T < T_C$ the profiles of the order parameter $\Delta\rho(z)$ follows the behaviour of an ordinary transition;
(ii) at $T > T_C$ the density profiles $\rho(z)$ follow the behaviour of a normal transition with preferential adsorption of voids.

The studies of the density profiles of the coexisting phases below T_C are not conclusive. Note also that, in agreement with the simulation results for LJ fluids [27], we never observed a

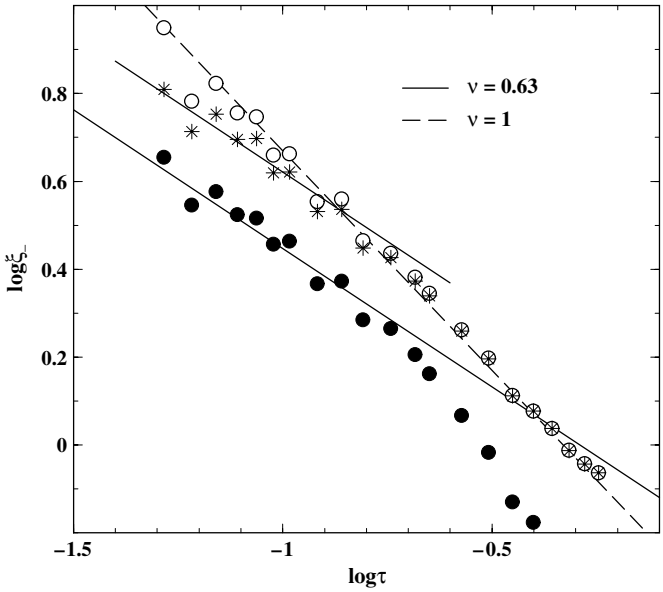

Figure 17. Correlation lengths along the coexistence curve of water in the slitlike pore with $H = 30$ Å, obtained from fitting equations (7) and (8) (solid circles) and equation (9) (open circles) to the order parameter profiles, and fitting equation (9) to the density profiles in the liquid phase (stars).

density minimum in case of a preferential adsorption of voids, which could be expected for small values of the surface field [21].

The definition of the local order parameter as the difference of the local densities of the coexisting phases, introduced in a way adopted for a bulk fluid, provides a vanishing order parameter at $T \geqslant T_C$ and therefore a flat profile $\Delta\rho(z) = 0$ at $T = T_C$. This assumes that the critical behaviour of the order parameter $\Delta\rho(z)$ belongs to the universality class of ordinary transition. Indeed, the temperature dependence of the order parameter in the surface layer, its temperature crossover in subsequent layers, and the shape of the order parameter profiles follow the behaviour of an ordinary transition.

The densities of the coexisting phases $\rho_{l,v}$ in general case could be written as

$$\rho_{l,v}(z, \tau) = \Delta\rho(z, \tau) + \rho_d(z, \tau), \tag{11}$$

where a symmetrical contribution is presented by the order parameter $\Delta\rho(z, \tau)$, while the asymmetric term $\rho_d(z, \tau)$ is the diameter, which contains regular as well as some singular terms. At the critical point the order parameter vanishes and the density profile reflects a preferential adsorption, which is described solely by the asymmetric term $\rho_d(z, \tau)$. We assume that equation (2) for the critical behaviour in the surface layer in the case of a normal transition below T_C describes the asymmetric contribution to the density profiles. So, the densities of the coexisting phases in the surface layer ($z = 0$) below T_C should behave in general as superposition of equations (1) and (2):

$$\rho_{l,v}(z = 0, \tau) = (\rho_{1C} + A_1\tau + A_2\tau^2 + \cdots) + B_-\tau^{2-\alpha} \pm B_1\tau^{\beta_1}. \tag{12}$$

In the case of coexisting bulk liquid and vapour phases ($z \to \infty$) the exponent $\beta_1 = 0.82$ in equation (12) should be replaced by $\beta = 0.326$, $\rho_C(z)$ by the bulk critical density ρ_{3D} and the exponent $(2 - \alpha)$ by the critical anomaly exponent of the diameter $(1 - \alpha)$ [83]. (Note that the

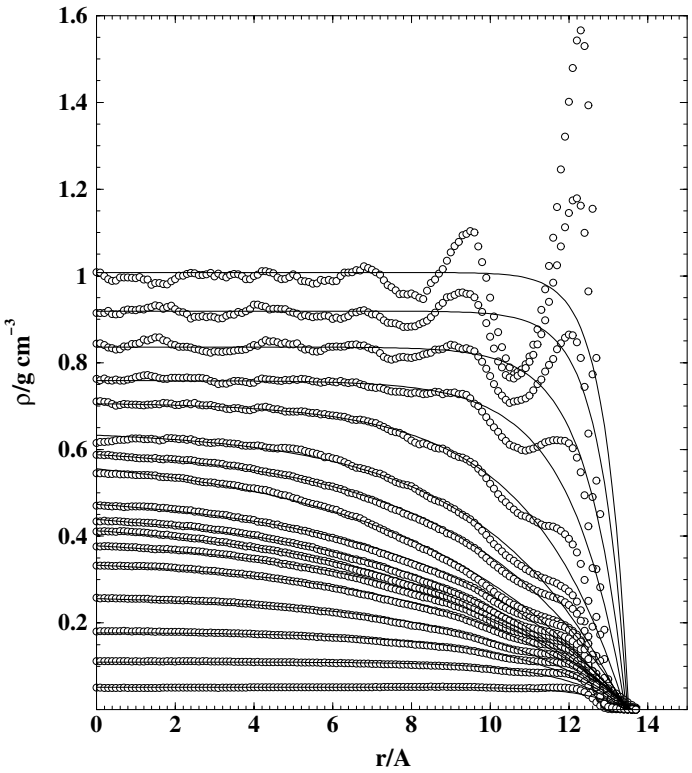

Figure 18. Density profiles of supercritical water in the slitlike pore with $H = 30$ Å at $T = 580$ K and at various average densities: from 0.047 g cm^{-3} (bottom) to 0.945 g cm^{-3} (top). The fits using equation (10) are shown by curves.

exponent $\alpha_{\rm ord}$ for the ordinary transition is $\alpha_{\rm ord} = \alpha - 1$ [59], providing $1 - \alpha_{\rm ord} = 2 - \alpha$.) The validity of the critical anomaly of a diameter $\tau^{(1-\alpha)}$ in fluids is questionable due to the so-called pressure mixing in the scaling fields, which generates a term $\tau^{2\beta}$ that could dominate the $\tau^{(1-\alpha)}$ term when $\tau \to 0$ [84].

To our knowledge, the temperature dependence of the difference between the magnetizations of the coexisting phases near the surface $\Delta m = (m_1 - m_2)/2$ has not been studied for the Ising model, when $h_1 \neq 0$. At any non-zero value of a surface field the Δm near the surface vanishes below $T_{\rm C}$ at the wetting transition temperature [2]. So, the occurrence of the wetting transition in the Ising model with short-range non-zero surface field h_1 and in some one-component fluids or fluid mixtures prevents an analysis of the asymptotic behaviour of the order parameter, defined as the difference between magnetizations (densities, concentrations) of the coexisting phases. We may assume that equation (12) is valid at least below the temperature of the wetting transition. This agrees with the available experimental studies of the local order parameter in binary mixtures [24, 25]. When the long-range fluid–wall interaction makes a wetting (drying) transition impossible at any $T < T_{\rm C}$ (the case studied in the present paper), equation (12) should be valid also asymptotically at $\tau \to 0$. There is only one solution of equation (12) above the temperature of the wetting transition. However, in this case the density of the liquid near the surface still includes both symmetric and asymmetric terms.

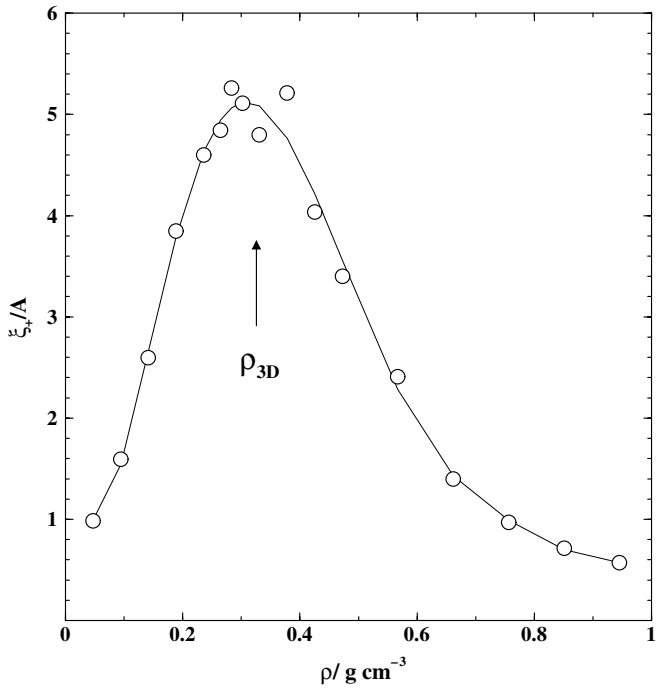

Figure 19. Effective values of the correlation length along the supercritical isotherm $T = 580$ K, obtained from the fit of the supercritical densities profiles, shown in figure 16, to equation (10) Critical density of the bulk TIP4P water $\rho_{3D} = 0.330$ g cm^{-3} [29] is shown by arrow. The curve is only a guide for the eyes.

Nevertheless, it is not clear whether equation (12) is valid for any value of h_1 or is valid in our studies due the small value of h_1. The extremely weak fluid–wall interaction (about 10% of fluid–fluid interaction) provides practically the strongest possible value h_1 for the preferential adsorption of voids for existing solid substrates. Assuming that the case $h_1 = 0$ is signalled by the flat density profile at the critical point [27], we can expect that equation (12) will be valid for the water–wall interactions with well-depths U_0 from -0.39 kcal mol^{-1} (present studies) to about -1.0 kcal mol^{-1} [29]. Further strengthening of the fluid–wall interaction causes a change of the sign of the surface field h_1 in favour of molecules. However, the possibility to increase this field is limited by the formation of dead layers at the wall [29], which are identical in both coexisting phases and, therefore, effectively form a new liquid-like wall. As a result the fluid–wall interaction comes close to the fluid–fluid interaction and is only slightly influenced by the interaction between the molecules and a solid wall. Note also that a possible change of h_1 with temperature [85] cannot be excluded and may complicate the study of the critical adsorption in one-component fluids [86, 87].

So, the presented study of water near a hydrophobic surface in a wide temperature range below T_C and in the supercritical region shows that the behaviour of the order parameter $\Delta\rho$ is described by the laws of the ordinary transition, while the behaviour of the asymmetric contribution to the densities of the liquid (ρ_l) and vapour (ρ_v) phases is consistent with the laws of the normal transition. Similar results were obtained for the LJ fluid near a weakly attractive substrate [88]. The surface critical behaviour of a one-component fluid for various strengths of fluid–wall interaction and in closer proximity to the bulk critical temperature definitely needs further investigations.

Acknowledgments

This work was supported by Deutsche Forschungsgemeinschaft. The authors thank K Binder, H W Diehl, S Dietrich and R Evans for stimulating discussions and useful advice.

References

[1] Cahn J W 1977 *J. Chem. Phys.* **66** 3667
[2] Nakanishi H and Fisher M E 1982 *Phys. Rev. Lett.* **49** 1565
[3] Pandit R, Schick M and Wortis M 1982 *Phys. Rev.* B **26** 5112
[4] Dietrich S 1988 *Phase Transitions and Critical Phenomena* vol 12, ed C Domb and J L Lebowitz (New York: Academic) p 1
[5] Henderson J R and van Swol F 1985 *Mol. Phys.* **56** 1313
[6] Stillinger F H 1972 *J. Solut. Chem.* **2** 141
[7] Lum K, Chandler D and Weeks J D 1999 *J. Phys. Chem.* B **103** 4570
[8] Brovchenko I, Geiger A and Oleinikova A 2002 *New Kinds of Phase Transitions: Transformations in Disordered Substances* (*Proc. NATO Advanced Research Workshop*) ed V V Brazhkin, S V Buldyrev, V N Rhyzhov and H E Stanley (Dordrecht: Kluwer) p 367
[9] Swol F and Henderson J R 1989 *Phys. Rev.* A **40** 2567
[10] Nijmeijer M J P, Bruin C, Bakker A F and van Leeuwen J M J 1991 *Phys. Rev.* B **44** 834
[11] Ebner C and Saam W F 1987 *Phys. Rev.* B **35** 1822
Ebner C and Saam W F 1987 *Phys. Rev. Lett.* **58** 587
[12] Nightingale M P and Indekeu J O 1985 *Phys. Rev.* B **32** 3364
[13] Hess G B, Sabatini M J and Chan M H W 1997 *Phys. Rev. Lett.* **78** 1739
[14] Binder K 1983 *Phase Transitions and Critical Phenomena* vol 8, ed C Domb and J L Lebowitz (London: Academic) p 1
[15] Binder K and Hohenberg P C 1972 *Phys. Rev.* B **6** 3461
Binder K and Hohenberg P C 1974 *Phys. Rev.* B **9** 2194
[16] Landau D P and Binder K 1990 *Phys. Rev.* B **41** 4633
[17] Diehl H W and Shpot M 1994 *Phys. Rev. Lett.* **73** 3431
[18] Guida R and Zinn-Justin J 1998 *J. Phys. A: Math. Gen.* **31** 8103
[19] Fisher M E and de Gennes P G 1978 *C. R. Acad. Sci.* B **287** 207
[20] Diehl H W 1994 *Ber. Bunsenges. Phys. Chem.* **98** 466
Diehl H W 1994 *Phys. Rev.* B **49** 2846
[21] Ritschel U and Czerner P 1996 *Phys. Rev. Lett.* **77** 3645
Ritschel U and Czerner P 1997 *Physica* A **237** 240
[22] Maciolek A, Ciach A and Drzewinski A 1999 *Phys. Rev.* E **60** 2887
[23] Law B 2001 *Prog. Surf. Sci.* **66** 159
[24] Sigl L and Fenzl W 1986 *Phys. Rev. Lett.* **57** 2191
Fenzl W 1993 *Europhys. Lett.* **24** 557
[25] Durian D J and Franck C 1987 *Phys. Rev. Lett.* **59** 555
[26] Cho J-H J and Law B 2001 *Phys. Rev.* E **65** 011601
[27] Maciolek A, Evans R and Wilding N B 2003 *J. Chem. Phys.* **119** 8663
[28] Brovchenko I, Geiger A and Oleinikova A 2001 *Phys. Chem. Chem. Phys.* **3** 1567
[29] Brovchenko I, Geiger A and Oleinikova A 2004 *J. Chem. Phys.* **120** 1958
[30] Evans R, Marini Bettolo Marconi U and Tarazona P 1986 *J. Chem. Soc. Faraday Trans.* 2 **82** 1763
[31] Cardy J L 1983 *J. Phys. A: Math. Gen.* **16** 3617
[32] Pleimling M and Selke W 1998 *Eur. Phys. J.* B **5** 805
Pleimling M 2004 *J. Phys. A: Math. Gen.* **37** R79
[33] Hanke A, Krech M, Schlesener F and Dietrich S 1999 *Phys. Rev.* E **60** 5163
[34] Igloi F, Peschel I and Turban L 1993 *Adv. Phys.* **42** 683
[35] Yu C-J, Richter A G, Datta A, Durbin M K and Dutta P 1999 *Phys. Rev. Lett.* **82** 2326
[36] Doerr A K, Tolan M, Seydel T and Press W 1998 *Physica* B **248** 263
Doerr A K, Tolan M, Schlomka J-P and Press W 2000 *Europhys. Lett.* **52** 330
[37] Thomas R K 2004 private communication
[38] Steitz R, Gutberlet T, Hauss T, Klosgen B, Krastev R, Schemmel S, Simonsen A C and Findenegg G H 2003 *Langmuir* **19** 2409
[39] Schwendel D, Hayashi T, Dahint R, Pertsin A, Grunze M, Streitz R and Schreiber F 2003 *Langmuir* **19** 2284

[40] Jensen T R, Jensen M O, Reitzel N, Balashev K, Peters G H, Kjaer K and Bjornholm T 2003 *Phys. Rev. Lett.* **90** 086101
[41] Lakshminarayanan V and Sur U K 2003 *Pramana J. Phys.* **61** 1739
[42] Attard P 2003 *Adv. Colloid Interface Sci.* **104** 75
[43] Yakubov G E, Butt H-J and Vinogradova O I 2000 *J. Phys. Chem.* **104** 3407
[44] Christenson H K and Claesson P M 2001 *Adv. Colloid Interface Sci.* **91** 391
[45] Evans R 1990 *J. Phys.: Condens. Matter* **2** 8989
[46] Berard D R, Attard P and Pattey G N 1993 *J. Chem. Phys.* **98** 7236
Attard P 1997 *J. Chem. Phys.* **107** 3230
[47] Dominguez H, Allen M P and Evans R 1999 *Mol. Phys.* **96** 209
[48] Noworyta J P, Henderson D and Sokolowski S 1999 *Mol. Phys.* **96** 1139
[49] Brovchenko I, Paschek D and Geiger A 2000 *J. Chem. Phys.* **113** 5026
Brovchenko I and Geiger A 2002 *J. Mol. Liq.* **96/97** 195
[50] Bratko D, Curtis R A, Blanch H W and Prausnitz J M 2001 *J. Chem. Phys.* **115** 3873
[51] Hayashi T, Pertsin A J and Grunze M 2002 *J. Chem. Phys.* **117** 6271
Pertsin A J, Hayashi T and Grunze M 2002 *J. Phys. Chem.* B **106** 12274
[52] Attard P, Ursenbach C P and Pattey G N 1992 *Phys. Rev.* A **45** 7621
[53] Forsman J, Jonsson Bo, Woodward C E and Wennerstrom H 1997 *J. Phys. Chem.* B **101** 4253
Forsman J, Woodward C E and Jonsson Bo 1997 *J. Colloid Interface Sci.* **195** 264
[54] Brodskaya E N, Zakharov V V and Laaksonen A 2002 *Colloid J.* **64** 538
[55] Rivera J L, McCabe C and Cummings P T 2002 *Nano Lett.* **2** 1427
[56] Salamacha L, Patrykiejew A, Sokolowski S and Binder K 2004 *J. Chem. Phys.* **120** 1017
[57] Jorgensen W L, Chandrasekhar J, Madura J D, Impey R W and Klein M L 1983 *J. Chem. Phys.* **79** 926
[58] Panagiotopoulos A Z 1987 *Mol. Phys.* **62** 701
[59] Diehl H W 1986 *Phase Transitions and Critical Phenomena* vol 10, ed C Domb and J L Lebowitz (London: Academic) p 75
[60] Binder K, Landau D P and Muller M 2003 *J. Stat. Phys.* **110** 1411
[61] Fisher M E and Nakanishi H 1981 *J. Chem. Phys.* **75** 5857
Nakanishi H and Fisher M E 1983 *J. Chem. Phys.* **78** 3279
[62] Evans R, Marconi Marini Bettolo U and Tarazona P 1986 *J. Chem. Phys.* **84** 2376
[63] Brovchenko I, Geiger A, Oleinikova A and Paschek D 2003 *Eur. Phys. J.* E **12** 69
[64] Binder K and Landau D P 1992 *J. Chem. Phys.* **96** 1444
[65] Ancilotto F, Curtarolo S, Toigo F and Cole M W 2001 *Phys. Rev. Lett.* **87** 206103
[66] Gao G T, Zeng X C and Tanaka H 2000 *J. Chem. Phys.* **112** 8534
[67] Fisher M E 1971 *Proc. Int. School of Physics 'Enrico Fermi' on Critical Phenomena* (New York: Academic) Course 51
[68] Binder K 1974 *Thin Solid Films* **20** 367
[69] Schilbe P, Siebentritt S and Rieder K-H 1996 *Phys. Lett.* A **216** 20
[70] Dillmann O, Janke W, Müller M and Binder K 2001 *J. Chem. Phys.* **114** 5853
[71] Mon K K and Binder K 1992 *J. Chem. Phys.* **96** 6989
[72] Jiang S and Gubbins K E 1995 *Mol. Phys.* **86** 599
[73] Bonetti M, Calmettes P and Bervillier C 2001 *J. Chem. Phys.* **115** 4660
[74] Reiter G F, Li J C, Mayers J, Abdul-Redah T and Platzman P 2004 *Braz. J. Phys.* **34** 142
[75] Vendruscolo M, Fasolino A and Rovere M 1993 *Nuovo Cimento* **15D** 541
[76] Selke W, Syalma F, Lajko P and Igloi F 1997 *J. Stat. Phys.* **89** 1079
[77] Pleimling M and Selke W 1998 *Eur. Phys. J.* B **1** 385
[78] Bengrine M, Benyoussef A, Ey-Zahraouy H and Mhirech F 1999 *Physica* A **268** 149
[79] Kumar P 1974 *Phys. Rev.* B **10** 2928
[80] Gomper G 1984 *Z. Phys.* B **56** 217
[81] Binder K, Stauffer D and Wildpaner V 1975 *Acta Metall.* **23** 1191
[82] Morita T, Kusano K, Ochiai H, Saitow K and Nishikawa K 2000 *J. Chem. Phys.* **112** 4203
[83] Mermin N D 1971 *Phys. Rev. Lett.* **26** 169
Rehr J J and Mermin N D 1973 *Phys. Rev.* A **8** 472
[84] Kim Y C, Fisher M E and Luijten E 2003 *Phys. Rev. Lett.* **91** 065701
[85] Kiselev S B, Ely J F and Belyakov M Yu 2000 *J. Chem. Phys.* **112** 2370
[86] Blumel S and Findenegg G H 1985 *Phys. Rev. Lett.* **54** 447
[87] Garcia R, Scheidemantel S, Knorr K and Chan M H W 2003 *Phys. Rev.* E **68** 056111
[88] Brovchenko I, Geiger A and Oleinikova A 2004 *Phys. Rev.* E submitted